Dynamics of electronic Rydberg wave packets in isolated-core excited atoms

O. Zobay and G. Alber
Theoretische Quantendynamik, Fakultät für Physik, Universität Freiburg, D-79104 Freiburg im Breisgau, Germany
(Received 26 January 1995)

Based on the concept of photon-dressed core states the influence of nonperturbative laser-induced isolated-core excitations on the time evolution of an excited electronic Rydberg wave packet is investigated. In this approach the shake-up process induced by Rabi oscillations of the ionic core is described as repeated scatterings of the excited wave packet between the channels associated with the dressed states of the ionic core. The corresponding scattering matrix and threshold energies of the dressed channels can be controlled externally by varying the laser parameters. The dependence of the wave-packet dynamics on the strength of the laser-induced core coupling and on the difference between the quantum defects of the two bare Rydberg series is worked out.

PACS number(s): 32.80.Rm, 32.80.Dz

I. INTRODUCTION

During the last ten years, the study of electronic Rydberg wave packets in atoms has made rapid progress in both theoretical and (due to the development of picosecond laser pulse techniques) in experimental aspects [1–10]. Work in this field of research is motivated mainly by the fact that these systems are situated on the border between microscopic and macroscopic physics and that their dynamics exhibits both quantum mechanical as well as classical aspects. This interplay between classical and quantum mechanical behavior has already been verified in various contexts. In studies of the dynamics of radial electronic Rydberg wave packets in pure Coulomb fields [2–7], for example, it has been shown that, though initially such a wave packet evolves similarly to a localized classical phase space distribution, quantum mechanical dispersion starts to dominate already after a few radial oscillations. The quantum nature of the time evolution of such wave packets shows up also in fractional and full revivals [8] which are caused by the discreteness of the electronic energy spectrum and which cannot be explained classically. Furthermore, studies of the dynamics of electronic Rydberg wave packets under the additional influence of external static fields [9,10] have shown that, although the electronic wave function tends to be concentrated along classically allowed paths, the characteristic quantum aspects manifest themselves in the interference of the associated probability amplitudes. All these dynamical aspects refer to the time evolution of a Rydberg electron far away from the positively charged ionic core.

Close to the nucleus (up to distances of typically a few Bohr radii), however, the dynamics of the Rydberg valence electron is determined by electron correlation effects and, possibly, by laser-induced processes. Electron correlations lead to scattering of the Rydberg electron by the ionic core and to autoionization. Laser-induced processes may affect a Rydberg electron either directly by causing it to absorb or emit a photon or indirectly by exciting a core electron and influencing the Rydberg electron through the resulting shakeup process [11]. This latter type of laser excitation, which has been termed isolated-core excitation (ICE), nowadays plays an important role as a spectroscopic tool, e.g., in studies of highly excited autoionizing states in two-electron-like atoms [12]. The idea of the ICE process consists of exciting initially an outer valence electron to a Rydberg state with one or several laser pulses and then inducing transitions in the positively charged ionic core by another laser pulse. Thereby, the Rydberg electron plays essentially the role of a spectator and is affected by the core transition only through the process of shakeup which leads to a change of its principal quantum number. This shakeup is made possible by a difference in the quantum defects of the two Rydberg series involved in the transition.

In connection with the dynamics of Rydberg wave packets ICE excitation processes have been studied so far in a series of three articles by Wang and Cooke [13–15] and in an article by Story, Duncan, and Gallagher [16]. In these studies, ICE by short and weak laser pulses is used as a means of preparing and examining autoionizing Rydberg wave packets. In particular, it has been shown that in this way shock waves and dark waves may be prepared and that the dependence of off-resonant ICE absorption on the position of the Rydberg electron may be investigated. However, these studies have so far concentrated only on cases in which the laser-induced transitions of the core electron are so weak that they can be described perturbatively. Nonperturbative effects of ICE excitations have been investigated recently by various groups [17–20]. In particular, Robicheaux [19] has studied their effect on the frequency dependence of photoabsorption cross sections. By using the concept of photon-dressed core states it was shown that photoabsorption cross sections are modified as soon as the Rabi frequency of the core transition exceeds the mean level spacing of the excited Rydberg state.

In the present article a theoretical description for the dynamics of an electronic Rydberg wave packet under the influence of nonperturbative laser-induced core transitions is developed. It is based on multichannel quan-

tum defect theory (MQDT) [21,22] and the concept of photon-dressed core states [19]. An analytical expression is derived for the relevant two-photon transition amplitude with which the dynamics of such an electronic Rydberg wave packet in a pump-probe-type experiment can be investigated. From this expression for the two-photon transition amplitude a semiclassical path representation is obtained which describes the time evolution of the excited Rydberg wave packet. It exhibits clearly that the shakeup process which is caused by laser-induced Rabi oscillations of the core leads to repeated scatterings of the wave packet between the channels which are associated with the dressed states of the ionic core. Furthermore, the threshold energies of the corresponding dressed channels are shifted due to the ac-Stark splitting of the resonantly coupled core states. Thus, the characteristic dynamical behavior of an electronic Rydberg wave packet under the influence of nonperturbative core transitions depends mainly on the magnitude of the Rabi period of the core transition in comparison with the orbit time of the excited wave packet and on the difference between the quantum defects of the channels associated with the laser-excited core states which determines the extent of the shakeup. In particular, it is shown that opposite to the situation in energy-resolved investigations [19] effects of nonperturbative laser-induced core transitions modify the dynamics of an excited electronic Rydberg wave packet significantly even if the Rabi frequency of the core transition is smaller than the mean level spacing of the excited Rydberg states.

This article is organized as follows. In Sec. II it is shown how, with the concept of photon-dressed core states, the time evolution of radial electronic Rydberg wave packets under the influence of nonperturbative laser-induced core transitions can be described. For the sake of simplicity the main ideas are introduced in part A for a model consisting only of two atomic channels which are coupled almost resonantly by laser-induced core transitions. Generalizations to multichannel excitation processes in the presence of laser-induced core transitions are presented in part B.

With the help of these theoretical results, in Sec. III we discuss the time evolution of a radial electronic Rydberg wave packet under the influence of laser-induced Rabi oscillations of the ionic core. Whereas part A concentrates on the description of pump-probe experiments with short and weak laser pulses, part B is devoted to the dynamics of depletion wave packets [1,23] which are prepared by a long and intense laser field through the mechanism of power broadening. The dependence of the energies of the dressed Rydberg states on the intensity of the cw-laser field is discussed in part C.

II. NONPERTURBATIVE ISOLATED-CORE EXCITATION OF RYDBERG SERIES

Based on the concept of photon-dressed core states [19] we give a detailed derivation of an analytical expression for the two-photon transition amplitude with which the influence of laser-induced core transitions on the time evolution of a radial electronic Rydberg wave packet can be studied. In part A the main ideas of this theoretical approach are introduced within a two-channel approximation. Generalizations to multichannel excitation processes are discussed in part B.

A. Isolated-core excitation in the two-channel approximation

In order to put the problem into perspective let us consider a typical isolated-core excitation (ICE) process involving an alkaline-earth atom, for example, as shown schematically in Fig. 1(a). Initially the atom is prepared in an energetically low lying bound state $|g\rangle$ with energy ε_g. The atom is situated in a cw-laser field

$$\mathbf{E}(t) = \mathcal{E}\mathbf{e}\, e^{-i\omega t} + \text{c.c.} \tag{1}$$

which is tuned near resonance with a transition of the positively charged ionic core. Typically electron correlations imply that as long as the atom remains in the initial state $|g\rangle$ this laser field is well detuned from any atomic transition. Therefore it has a negligible effect on the atomic dynamics. But as soon as an outer atomic valence electron is excited to Rydberg states close to threshold the cw-laser field starts to induce transitions between the two resonantly coupled states of the ionic core which have energies ε_1 and ε_2, respectively. In the following only intensities I of the laser field $\mathbf{E}(t)$ are considered which are small in comparison with the atomic unit, i.e., $I \ll 10^{17}\ \mathrm{W\,cm^{-2}}$. In this case, effects of laser-induced transitions of the excited Rydberg electron to continuum states well above threshold, which could take place in addition to core transitions, are expected to be small and will be neglected in the following. However, they can be incorporated in the following formalism easily with the help of intensity dependent quantum defects [23].

We shall concentrate in the following mainly on cases in which the valence electron is excited coherently to the Rydberg states by a short and weak laser pulse:

$$\mathbf{E}_1(t) = \mathcal{E}_1(t)\mathbf{e}_1 e^{-i\omega_1 t} + \text{c.c.}\ , \tag{2}$$

where $\mathcal{E}_1(t)$ is a Gaussian-shaped envelope centered around time t_1 with pulse duration τ_1. This implies that a radial electronic Rydberg wave packet is generated by this short laser pulse. The wave packet moves in the Coulomb field of the positively charged ionic core. When-

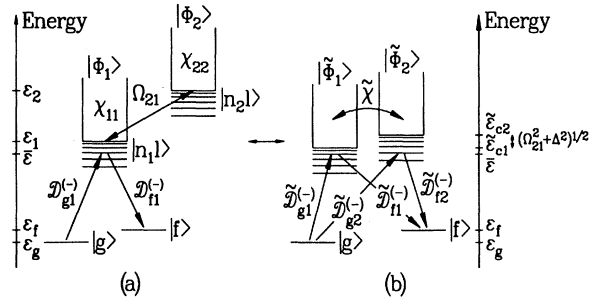

FIG. 1. Excitation scheme for the two-channel model: (a) bare Rydberg series, (b) "dressed" Rydberg series.

ever it penetrates the core region it is shaken up by the Rabi oscillations of the almost resonantly coupled ionic core states. Effects of this shakeup process on the dynamics of the electronic Rydberg wave packet may be probed, for example, by a second time-delayed short laser pulse (frequency ω_2, polarization $\mathbf{e}_2$, pulse duration τ_2) which is centered around time t_2 and which induces transitions to an energetically low lying bound atomic state $|f\rangle$ with energy ε_f. Typically this final state is not identical with the initial state $|g\rangle$. For the sake of simplicity let us assume in the following that the envelopes of pump and probe pulse are identical and that $\varepsilon_g + \omega_1 = \varepsilon_f + \omega_2 = \bar{\varepsilon}$.

Thus in the lowest order perturbation theory with respect to the pump and probe pulse the probability of observing after the interaction with both laser pulses the atom in state $|f\rangle$ is given by [1,24]

$$|\langle f \mid \Psi\rangle_{t\to\infty}|^2 = \left|\frac{1}{2\pi}\int_{-\infty}^{\infty} d\varepsilon \left|\tilde{\mathcal{E}}_1(\varepsilon-\bar{\varepsilon})\right|^2 T_{fg}(\varepsilon) e^{-i(\varepsilon-\bar{\varepsilon})(t_2-t_1)}\right|^2 \quad (3)$$

provided $|t_2 - t_1| \gg \tau_1, \tau_2$ (Hartree atomic units are used). The Fourier transforms of the envelope functions of pump and probe pulse are denoted by

$$\tilde{\mathcal{E}}_k(\varepsilon) = \int_{-\infty}^{\infty} dt\, \mathcal{E}_k(t) e^{i\varepsilon(t-t_k)}. \quad (4)$$

The two-photon transition amplitude

$$T_{fg}(\varepsilon) = \left\langle f \left| \mathbf{d}\cdot\mathbf{e}_2^* \frac{1}{\varepsilon - H + i0} \mathbf{d}\cdot\mathbf{e}_1 \right| g \right\rangle, \quad (5)$$

with $\mathbf{d}$ the atomic dipole operator, describes the response of the atom in the intense cw-laser field $\mathbf{E}(t)$ to pump and probe pulse. Thereby, the Hamiltonian operator H characterizes the dynamics in the excited atomic channels under the influence of the intense cw-laser field $\mathbf{E}(t)$. In the dipole and rotating wave approximation it is given by

$$H = H_1 + H_2 + V_{ICE}. \quad (6)$$

The Hamiltonians

$$H_j = (\mathbf{h}_{jj} + \mathbf{V}_{jj}(\rho) + \varepsilon_{cj}) |\Phi_j\rangle \langle\Phi_j| \quad (7)$$

describe the electronic dynamics in the bare atomic channels 1 and 2 in the absence of the cw-laser field. The channel states $|\Phi_j\rangle$ represent the state of the ionic core as well as the spin and the angular wave function of the excited Rydberg electron [1,21]. The radial Hamiltonian for the Rydberg electron in channel j with angular momentum l_j is given by $[\mathbf{h}_{jj} + \mathbf{V}_{jj}(\rho)]$ with $\mathbf{h}_{jj} = -\frac{1}{2}\frac{d^2}{d\rho^2} + \frac{l_j(l_j+1)}{2\rho^2} - \frac{1}{\rho}$ and $\mathbf{V}_{jj}(\rho)$ the short-range potential which describes effects of the residual core electrons. The radial coordinate of the Rydberg electron is denoted by ρ. As the excited channels have opposite parities there is no configuration interaction potential $V_{12}(\rho)$ coupling the two channels. In an ICE transition the angular momentum of the Rydberg electron is conserved so that $l_1 = l_2 = l$ [11,12]. The channel thresholds in the RWA are given by $\varepsilon_{c1} = \varepsilon_1$, $\varepsilon_{c2} = \varepsilon_2 - \omega$. According to standard treatments of ICE processes [13–16,25,26] the laser-induced coupling of the two channels may be modeled in the form

$$V_{ICE} = -\tfrac{1}{2}\Omega_{21}\left(|\Phi_1\rangle\langle\Phi_2| + |\Phi_2\rangle\langle\Phi_1|\right) \quad (8)$$

with the real-valued Rabi frequency of the core transition

$$\Omega_{21} = 2\,\langle\Phi_2|\,\mathbf{d}\cdot\mathbf{e}\,\mathcal{E}\,|\Phi_1\rangle\,. \quad (9)$$

The main problem in the theoretical description of nonperturbative ICE transitions is thus the determination of the two-photon transition amplitude. This goal may be achieved with the help of the Dalgarno-Lewis method [27] by solving the inhomogeneous Schrödinger equation

$$(\varepsilon - H + i0)\,|\lambda(\varepsilon)\rangle = \mathbf{d}\cdot\mathbf{e}_1\,|g\rangle \quad (10)$$

from which the two-photon transition amplitude is obtained by the relation

$$T_{fg}(\varepsilon) = \langle f\,|\mathbf{d}\cdot\mathbf{e}_2^*|\,\lambda(\varepsilon)\rangle\,. \quad (11)$$

The inhomogeneous Schrödinger equation can be solved with the help of methods of quantum defect theory (QDT) [21]. For this purpose we adopt an ansatz of the form

$$\langle\Omega,\rho\,|\lambda(\varepsilon)\rangle = \sum_{j=1,2} \Phi_j(\Omega) F^{(j)}(\rho;\varepsilon)/\rho. \quad (12)$$

The channel coordinates Ω represent the coordinates of the core electrons and the angular momentum and spin of the excited Rydberg valence electron. The radial part of the wave function of the excited Rydberg valence electron in channel j is denoted by $F^{(j)}(\rho;\varepsilon)$. Projection of Eq. (10) onto the normalized channel states $|\Phi_j\rangle$ yields

$$[\varepsilon - (\mathbf{h} + \boldsymbol{\varepsilon}_c + \mathbf{V}(\rho)) + \tfrac{1}{2}\boldsymbol{\Omega}_{21}]\mathbf{F}(\rho;\varepsilon) = \mathbf{D}(\rho) \quad (13)$$

with Im $\varepsilon = +0$. The 2×2 matrices $\mathbf{h}$, $\mathbf{V}$, $\boldsymbol{\varepsilon}_c$, and $\boldsymbol{\Omega}_{21}$ are obtained in an obvious way from Eqs. (7) and (8). The components of the column vector $\mathbf{F}(\rho;\varepsilon)$ are the radial wave functions of the Rydberg valence electron $F^{(j)}(\rho;\varepsilon)$. The laser-induced coupling between state $|g\rangle$ and the excited channels is described by the column vector $\mathbf{D}(\rho)$ with matrix elements $D_j(\rho) = \rho\int d\Omega\,\Phi_j^*(\Omega)\mathbf{d}\cdot\mathbf{e}_1\,\langle\Omega,\rho|\,g\rangle$. In the excitation scheme under consideration the coupling between $|g\rangle$ and channel 2 may be neglected $[D_2(\rho) = 0]$. We can assume $V_j(\rho) \simeq 0$ and $D_1(\rho) \simeq 0$ for $\rho \geq \rho_c$ with a typical core radius ρ_c of the order of a few Bohr radii [21,22]. In the close-coupling equations (13) the laser-induced interaction between both channels appears as a long-range interaction independent of the radial coordinate ρ of the Rydberg valence electron.

In order to determine the two-photon transition amplitude we subject Eq. (13) to the orthogonal transformation

$$\mathbf{O} = \begin{pmatrix} \cos\varphi & -\sin\varphi \\ \sin\varphi & \cos\varphi \end{pmatrix} \quad (14)$$

which is defined by the eigenvalue relation

$$\mathbf{O}^T(\boldsymbol{\varepsilon}_c - \tfrac{1}{2}\boldsymbol{\Omega}_{21})\mathbf{O} = \tilde{\boldsymbol{\varepsilon}}_c. \tag{15}$$

The 2×2 matrix $\mathbf{O}$ describes the transformation between the bare core channel states $|\Phi_j\rangle$ and the corresponding photon-dressed core channel states [19]. The diagonal matrix $\tilde{\boldsymbol{\varepsilon}}_c$ defines the dressed energies of the ionic core. Explicitly these dressed energies are given by $(\tilde{\boldsymbol{\varepsilon}}_c)_{11} \equiv \tilde{\varepsilon}_{c1} = \varepsilon - \frac{1}{2}\Omega_{21}\tan\varphi$ and $(\tilde{\boldsymbol{\varepsilon}}_c)_{22} \equiv \tilde{\varepsilon}_{c2} = \varepsilon + \frac{1}{2}\Omega_{21}\cot\varphi$. The corresponding rotation angle φ is defined by the relation $\tan(2\varphi) = \Omega_{21}/\Delta$ with the detuning $\Delta = \varepsilon_{c2} - \varepsilon_{c1}$. Applying this transformation to the inhomogeneous Schrödinger equation (13) yields

$$\{\varepsilon - [\mathbf{h} + \tilde{\boldsymbol{\varepsilon}}_c + \tilde{\mathbf{V}}(\rho)]\}\tilde{\mathbf{F}}(\rho;\varepsilon) = \tilde{\mathbf{D}}(\rho) \tag{16}$$

with the transformed configuration interaction matrix $\tilde{\mathbf{V}}(\rho) = \mathbf{O}^T\mathbf{V}(\rho)\mathbf{O}$. The corresponding transformed state vector of the Rydberg valence electron and the transformed dipole couplings are given by $\tilde{\mathbf{F}}(\rho;\varepsilon) = \mathbf{O}^T\mathbf{F}(\rho;\varepsilon)$ and $\tilde{\mathbf{D}}(\rho) = \mathbf{O}^T\mathbf{D}(\rho)$, respectively.

Equation (16) shows that as far as the dressed channels are concerned the long-range coupling contained in Eq. (13) causes two effects: it leads to an energy shift of the ionizations thresholds—which is due to the ac-Stark splitting of the dressed ionic core states—and it induces a short-range coupling between the dressed channels which is described by the transformed configuration interaction $\tilde{\mathbf{V}}(\rho)$. Outside the ionic core, i.e., for $\rho \geq \rho_c$, this coupling vanishes. As Eq. (16) contains only a short-range coupling between the dressed channels the two-photon transition amplitude can be obtained from it with the help of methods of MQDT [21,28]. It has been shown that for such a system of close coupled equations the transition amplitude can be written in the form [1,24]

$$T_{fg}(\varepsilon) = T_{fg}^{(s)} - 2\pi i \sum_{i,j\in c} \tilde{\mathcal{D}}_{fj}^{(-)}(\tilde{\boldsymbol{\chi}} - e^{-2\pi i\tilde{\boldsymbol{\nu}}})_{ji}^{-1}\tilde{\mathcal{D}}_{gi}^{(-)} \qquad (\mathrm{Im}\ \varepsilon = +0) \tag{17}$$

with an appropriately chosen dressed scattering matrix $\tilde{\boldsymbol{\chi}}$ and (energy normalized) photoionization dipole matrix elements $\tilde{\mathcal{D}}_{gj}^{(-)}$ and $\tilde{\mathcal{D}}_{fj}^{(-)}$ which describe radiative transitions between states $|g\rangle$ and $|f\rangle$ and the closed dressed channel j. Because of the short-range coupling between the dressed channels the quantities $T_{fg}^{(s)}$ (with $\mathrm{Im}\ T_{fg}^{(s)} = -\pi\sum_{j=1,2}|\tilde{\mathcal{D}}_{gj}^{(-)}\tilde{\mathcal{D}}_{fj}^{(-)}|$), $\tilde{\boldsymbol{\chi}}$, $\tilde{\mathcal{D}}_{gj}^{(-)}$, and $\tilde{\mathcal{D}}_{fj}^{(-)}$ are smooth functions of energy across any threshold [1,21,23,28,29]. The diagonal 2×2 matrix $e^{-2\pi i\tilde{\boldsymbol{\nu}}}$ has elements

$$(e^{-2\pi i\tilde{\boldsymbol{\nu}}})_{jj} = \exp\{-2\pi i[2(\tilde{\varepsilon}_{cj} - \varepsilon)]^{-1/2}\}.$$

The sum in Eq. (17) extends over all closed channels c with $\varepsilon < \tilde{\varepsilon}_{cj}$.

For the evaluation of the two-photon transition amplitude the analytical form of the dressed scattering matrix $\tilde{\boldsymbol{\chi}}$ and the dressed energy normalized dipole matrix elements remains to be determined. For this purpose we introduce for the Schrödinger equation in the absence of the intense cw-laser field, i.e.,

$$\{\varepsilon - [\mathbf{h} + \boldsymbol{\varepsilon}_c + \mathbf{V}(\rho)]\}\boldsymbol{\mathcal{F}}(\rho;\varepsilon) = 0, \tag{18}$$

the following fundamental system of energy normalized regular solutions which is given by

$$\{\varepsilon - [\mathbf{h}_{jj} + \varepsilon_{cj} + \mathbf{V}_{jj}(\rho)]\}\mathcal{F}_{jj}(\rho;\varepsilon) = 0$$
$$\mathcal{F}_{12}(\rho;\varepsilon) = \mathcal{F}_{21}(\rho;\varepsilon) \equiv 0 \tag{19}$$

with $j = 1, 2$. Asymptotically for $\rho \to \infty$ these solutions behave as

$$\mathcal{F}_{jk}(\rho;\varepsilon) \simeq s_l(\rho;\varepsilon - \varepsilon_{cj})\delta_{jk} + c_l(\rho;\varepsilon - \varepsilon_{cj})\tan(\pi\mu_j)\delta_{jk} \tag{20}$$

where $s_l(\varepsilon)$ and $c_l(\varepsilon)$ are the real-valued, energy-normalized regular and irregular Coulomb functions with energy ε and angular momentum $l = l_1 = l_2$ [1,21]. Thereby it has been taken into account that the short–range potential $\mathbf{V}(\rho)$ does not couple channels 1 and 2. The quantum defects of the excited channels are denoted μ_j.

Following the arguments of Robicheaux [19] in terms of these solutions an approximate fundamental system of regular solutions of the homogeneous part of Eq. (16) for the energy region above both thresholds is given by

$$\tilde{\mathcal{F}}_{jk}(\rho;\varepsilon) = \sum_{i,l=1,2} \mathbf{O}_{ji}^T\mathcal{F}_{il}(\rho;\varepsilon + \varepsilon_{ci} - \tilde{\varepsilon}_{cj})\mathbf{O}_{lk} \tag{21}$$

with $\tilde{\mathcal{F}}_{jk}$ the jth vector component of the kth solution $(j, k = 1, 2)$. The insertion of this ansatz into the left hand side of Eqs. (16) yields

$$(\varepsilon - \mathbf{h}_{jj} - \tilde{\varepsilon}_{cj})\tilde{\mathcal{F}}_{jk}(\rho;\varepsilon) - \sum_{m=1,2}\tilde{\mathbf{V}}(\rho)_{jm}\tilde{\mathcal{F}}_{mk}(\rho;\varepsilon)$$
$$= \sum_{l,m,n,p=1}^{N} \mathbf{O}_{jm}^T[\mathbf{V}(\rho)\mathbf{O}]_{ml}\mathbf{O}_{ln}^T[\mathcal{F}_{np}(\rho;\varepsilon + \varepsilon_{cm} - \tilde{\varepsilon}_{cj})$$
$$-\mathcal{F}_{np}(\rho;\varepsilon + \varepsilon_{cn} - \tilde{\varepsilon}_{cl})]\mathbf{O}_{pk}. \tag{22}$$

For $\rho > \rho_c$ the right hand side of Eq. (22) vanishes because outside the core region the core potentials $\mathbf{V}(\rho)$ vanish. For $\rho \leq \rho_c$ the right hand side is close to zero because the difference between the solutions $\mathcal{F}_{np}(\rho;\varepsilon + \varepsilon_{cm} - \tilde{\varepsilon}_{cj})$ and $\mathcal{F}_{np}(\rho;\varepsilon + \varepsilon_{cn} - \tilde{\varepsilon}_{cl})$ is small. This difference can be estimated semiclassically to be of the order of $(\rho_c^{3/2}\max\{|\Delta|, |\Omega_{21}|\})$ [29]. For typical core radii of a few Bohr radii and laser intensities I much less than the atomic unit of intensity, i.e., $I \ll 10^{17}\ \mathrm{W\,cm^{-2}}$, this difference is vanishingly small. Therefore, to a good degree of approximation a fundamental system of regular solutions of the homogeneous part of of Eq. (16) is given by Eq. (21). Asymptotically for $\rho \to \infty$ these solutions behave as

$$\tilde{\mathcal{F}}_{jk}(\rho;\varepsilon) \simeq \delta_{jk}s_l(\rho;\varepsilon - \tilde{\varepsilon}_{cj}) + c_l(\rho;\varepsilon - \tilde{\varepsilon}_{cj})\tilde{\boldsymbol{\mathcal{R}}}_{jk} \tag{23}$$

with the dressed reactance matrix [21]

$$\tilde{\boldsymbol{\mathcal{R}}} = \mathbf{O}^T\begin{pmatrix}\tan(\pi\mu_1) & 0\\ 0 & \tan(\pi\mu_2)\end{pmatrix}\mathbf{O}. \tag{24}$$

Consequently, one finds for the dressed scattering matrix

the expression [21]

$$\tilde{\boldsymbol{\chi}} = (\mathbf{1} + i\tilde{\boldsymbol{\mathcal{R}}})(\mathbf{1} - i\tilde{\boldsymbol{\mathcal{R}}})^{-1} = \mathbf{O}^T\boldsymbol{\chi}\mathbf{O} \tag{25}$$

with the bare scattering matrix

$$\boldsymbol{\chi} = \begin{pmatrix} e^{2\pi i\mu_1} & 0 \\ 0 & e^{2\pi i\mu_2} \end{pmatrix}. \tag{26}$$

Correspondingly, the (energy normalized) dressed photoionization dipole matrix element is given by [23,28]

$$\begin{aligned}\tilde{\boldsymbol{\mathcal{D}}}_g^{(-)} &= -\frac{i}{2}(\mathbf{1} + \tilde{\boldsymbol{\chi}}) \int d\rho\, \tilde{\boldsymbol{\mathcal{F}}}^T(\rho;\varepsilon) \begin{pmatrix} \tilde{D}_1(\rho) \\ \tilde{D}_2(\rho) \end{pmatrix} \\ &= \mathbf{O}^T\boldsymbol{\mathcal{D}}_g^{(-)}\end{aligned} \tag{27}$$

with the approximately energy independent and energy normalized photoionization dipole matrix elements $\boldsymbol{\mathcal{D}}_g^{(-)} = (\mathcal{D}_{g1}^{(-)}, 0)$ describing transitions from state $|g\rangle$ to the bare excited channel 1. An analogous expression holds for $\boldsymbol{\mathcal{D}}_f^{(-)}$. Inserting Eqs. (25) and (27) into Eq. (17) yields the final expression for the two-photon transition amplitude.

Equations (17), (25), and (27) show in a simple way how the laser-induced coupling of the core states modifies the characteristics of the Rydberg series involved. On the one hand the bare quantities $\boldsymbol{\chi}$ and $\mathcal{D}_{gj}^{(-)}$, $\mathcal{D}_{fj}^{(-)}$, which would appear in the two-photon transition amplitude in the absence of the laser-induced core coupling, are replaced by the corresponding dressed quantities $\tilde{\boldsymbol{\chi}}$ and $\tilde{\mathcal{D}}_{gj}^{(-)}$, $\tilde{\mathcal{D}}_{fj}^{(-)}$. Therefore, an appropriate choice of the parameters which characterize this laser-induced coupling, i.e., detuning Δ and Rabi frequency Ω_{21}, may lead to unusual scattering matrices which have large off-diagonal matrix elements. The resulting physical implications will be discussed in Sec. III in more detail. The orthogonal matrix $\mathbf{O}$ depends on the rotation angle φ and mediates the transformation between the bare core states (Φ_1, Φ_2) and the corresponding dressed states $(\tilde{\Phi}_1, \tilde{\Phi}_2)$, i.e., $(\Phi_1, \Phi_2)\mathbf{O} = (\tilde{\Phi}_1, \tilde{\Phi}_2)$. The mixing of the core states is thus transferred in a simple way to the Rydberg series. In addition, the energies of the thresholds of the series are shifted to the values of the dressed core states. These shifts are taken into account in the diagonal matrix $e^{-2\pi i\tilde{\boldsymbol{\nu}}}$.

The validity of Eqs. (17), (25), and (27) can easily be checked numerically. To this end, we write the two-photon transition amplitude in the form

$$\begin{aligned}T_{fg}(\varepsilon) = \langle f|\mathbf{d}\cdot\mathbf{e}_2^*[\varepsilon - H_1 \\ -V_{ICE}[\varepsilon - H_2]^{-1}V_{ICE}]^{-1}\mathbf{d}\cdot\mathbf{e}_1|g\rangle.\end{aligned} \tag{28}$$

This expression can now be calculated numerically by means of an eigenstate expansion if one makes use of the overlap formula for radial Rydberg wave functions [25], i.e.,

$$\langle n_1|\, n_2\rangle = (-1)^{n_2-n_1}\frac{2\sqrt{n_2^* n_1^*}}{n_1^* + n_2^*}\frac{\sin\pi(n_2^* - n_1^*)}{\pi(n_2^* - n_1^*)} \tag{29}$$

with the effective quantum numbers $n_j^* = n_j - \mu_j$.

If both Rydberg series have the same quantum defect the two-photon transition amplitude can be evaluated even analytically from Eq. (28) yielding a result identical to the corresponding special case of Eq. (17). If the quantum defects differ from each other this computation has to be performed numerically. In Fig. 2 both methods of computing the two-photon transition amplitude are compared with each other. The dots are computed with the use of Eqs. (28) and (29) and the full curve shows the corresponding result from Eq. (17) for a case in which $\mu_2 - \mu_1 = 0.32$ and the Rabi frequency $|\Omega_{21}|$ is larger than the mean level spacing of the excited Rydberg states. The good agreement between the two calculations is also observed for other parameter values. This confirms the validity of Eqs. (17), (25), and (27) and further justifies the approximation for the fundamental system of solutions given in Eq. (21) as the starting point for its derivation.

Perturbative theoretical descriptions of ICE transitions are recovered in the limit $|\varphi| \approx |\Omega_{21}/2\Delta| \ll 1$ [19]. For example, assume that Rydberg series 2 is slightly autoionizing and consider the following typical situation from energy-resolved spectroscopy: A first weak cw-laser with amplitude $\mathcal{E}_1$ and frequency ω_1 couples the initial state $|g\rangle$ almost resonantly to a Rydberg state $|n_1\rangle$ in channel 1. A second weak cw-laser couples $|n_1\rangle$ to states $|\nu_2\rangle$ in the autoionizing channel 2 with energies $\varepsilon_{\nu_2} = \varepsilon_2 - 1/(2\nu_2^2)$. Modeling the autoionizing character of the Rydberg series in channel 2 by a complex quantum defect $\mu_2 + i\eta$ with the scaled autoionization linewidth 2η the depletion rate Γ of the initial state $|g\rangle$ is given by $\Gamma = -2\,|\mathcal{E}_1|^2\,\mathrm{Im}\,T_{gg}(\varepsilon_g + \omega_1)$ according to Fermi's golden rule. For this quantity one obtains from Eq. (17) in the limit $|\varphi| \approx |\Omega_{21}/2\Delta| \ll 1$ and $\eta \ll 1$

$$\begin{aligned}\Gamma = &\frac{2\pi^2(\Omega_1/2)^2}{\sin^2\pi(\nu_1 + \mu_1)} \\ &\times(\Omega_{21}/2)^2\frac{\eta}{|\sin\pi(\nu_2 + \mu_2 + i\eta)|^2}\frac{\sin^2\pi(\nu_1 - \nu_2)}{\Delta^2}\end{aligned} \tag{30}$$

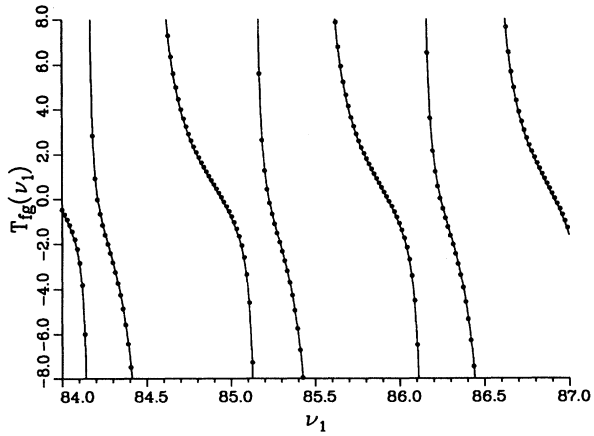

FIG. 2. Comparison between calculations of the two-photon transition amplitude (in units of $|\mathcal{D}_{g1}^{(-)}\mathcal{D}_{f1}^{(-)}|$) according to Eq. (17) (full lines) and Eqs. (28) and (29) (dots), respectively, for the parameters $\mu_1 = 0.0$, $\mu_2 = 0.32$, $\Omega_{21} = 2.0\times10^{-6}$ a.u., $\Delta = 0$, Re $T_{fg}^{(s)} = 0$, and $\nu_1 = [2(\varepsilon_1 - \varepsilon)]^{-1/2}$.

with the Rabi frequency of the transition $|g\rangle \rightarrow |n_1\rangle$ denoted by Ω_1. Thereby the effective quantum number ν_1 is related to the excited energy in channel 1 by $\varepsilon_g + \omega_1 = \varepsilon_1 - 1/(2\nu_1^2)$. Thus for ν_1 fixed the ansatz presented in Ref. [15] for the ν_2 dependence of the transition rate between the Rydberg series is recovered which we have not used in our derivation. For $|\nu_1 - \nu_2| \ll \nu_1$ and $0 < |\nu_1 + \mu_1 - n_1| \ll 1$ the above expression can be cast into the form

$$\Gamma = \left\{ \frac{(\Omega_1/2)^2 \nu_1^{-3}}{(\varepsilon_{n_1} - \varepsilon_g - \omega_1)^2} \right\} \times \left\{ (\Omega_{21}/2)^2 2\pi \frac{\nu_2^3 \pi \eta}{|\sin^2[\pi(\nu_2 + \mu_2 + i\eta)]|} \times \frac{\sin^2[\pi(\nu_1 - \nu_2)]}{\pi^2(\nu_1 - \nu_2)^2} \right\}. \quad (31)$$

Here, the first term in curly brackets can be interpretated as the probability of (almost resonant) excitation of the bound Rydberg state $|n_1\rangle$ from the initial state $|g\rangle$. According to the Golden rule the second term describes one-photon excitation of the autoionizing channel states $|\nu_2\rangle$ from the bound Rydberg state $|n_1\rangle$.

B. Multichannel excitation processes in the presence of laser-induced core transitions

Now we generalize our previous discussion to the case of multichannel excitation processes in the presence of laser-induced core transitions. More specifically, we consider short-pulse excitation from a low-lying initial state into a group of Coulomb fragmentation (free) channels which may be coupled to further free channels by electron correlations and by laser-induced excitations of the ionic core. Thereby the laser-induced excitations of the core can arise from one or several cw-laser fields. An example of a possible excitation process of this kind is shown in Fig. 3. Again the main problem in the theoretical description of the dynamics of the excited Rydberg electron is the determination of the two-photon transition amplitude. It is defined by an expression analogous to Eq. (5) where now the Hamiltonian H describes the almost resonant laser-induced excitation of the ionic core states as well as configuration interaction induced couplings between (free) channels of the Rydberg valence electron.

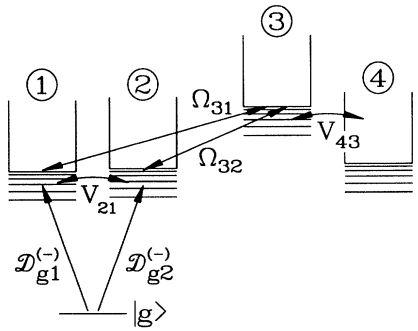

FIG. 3. Example of a multichannel excitation process which can be analyzed with the help of the methods derived in Sec. II B. The initial state $|g\rangle$ is excited to two free channels 1 and 2 which are coupled to each other by configuration interaction. These channels are further coupled through ICE transitions to channel 3 which can autoionize into channel 4. The relevant components of $\mathcal{D}_g^{(-)}$, $\mathbf{V}$, and $\mathbf{\Omega}$ are also indicated. The de-excitation to state $|f\rangle$ is not shown.

For the evaluation of the transition amplitude we adopt the ansatz

$$\langle \Omega, \rho \, | \lambda(\varepsilon) \rangle = \sum_{j=1}^{N} \Phi_j(\Omega) F^{(j)}(\rho;\varepsilon)/\rho. \quad (32)$$

Projecting the inhomogeneous Schrödinger equation analogous to Eq. (10) onto the N core states $|\Phi_j\rangle$ the following system of close-coupled equations is obtained for the radial wave function $\mathbf{F}(\rho;\varepsilon)$ of the Rydberg valence electron

$$[\varepsilon - (\mathbf{h} + \boldsymbol{\varepsilon}_c + \mathbf{V}(\rho)) + \tfrac{1}{2}\mathbf{\Omega}]\mathbf{F}(\rho;\varepsilon) = \mathbf{D}(\rho) \quad (33)$$

with Im ε=+0. The diagonal $N \times N$ matrix $\mathbf{h}$ is given by $\mathbf{h}_{jj} = -\frac{1}{2}\frac{d^2}{d\rho^2} + \frac{l_j(l_j+1)}{2\rho^2} - \frac{1}{\rho}$ with the angular momentum l_j of the excited Rydberg valence electron in channel j. For convenience, we assume in the following that the (free) channels are grouped according to the possible values of the angular momentum of the excited Rydberg electron, i.e., $l_i = l_1$ for $i = 1, ..., N_1$, $l_i = l_{N_1+1}$ for $i = N_1+1, ..., N_2$, etc. As in Eq. (13) the diagonal $N \times N$ matrix $\boldsymbol{\varepsilon}_c$ is defined by the ionization thresholds of the bare channels of the excited Rydberg valence electron which are shifted appropriately by the photon energies of the corresponding dressing laser fields. The Hermitian $N \times N$ matrix $\mathbf{V}(\rho)$ describes the short-range configuration interaction which originates from the presence of the residual core electrons. Analogous to Eq. (9) the Hermitian $N \times N$ matrix $\mathbf{\Omega}$ describes the coupling between core states of different parities induced by the cw-laser fields. As the angular momentum of the Rydberg valence electron remains unchanged during a radiative transition of the ionic core [11,21], our enumeration of the channels implies that the matrix $\mathbf{\Omega}$ is blockdiagonal. The N dimensional column vector $\mathbf{D}(\rho)$ describes excitation of the Rydberg valence electron from the initially prepared state $|g\rangle$.

For the derivation of an analytical expression for the two-photon transition amplitude $T_{fg}(\varepsilon)$ we start from the fundamental system of regular solutions $\boldsymbol{\mathcal{F}}(\rho;\varepsilon)$ of the Schrödinger equation in the absence of laser-induced core transitions, i.e.,

$$\{\varepsilon - [\mathbf{h} + \boldsymbol{\varepsilon}_c + \mathbf{V}(\rho)]\}\boldsymbol{\mathcal{F}}(\rho;\varepsilon) = 0. \quad (34)$$

Asymptotically for $\rho \rightarrow \infty$ these solutions behave as

$$\mathcal{F}_{jk}(\rho;\varepsilon) \rightarrow s_{l_j}(\rho;\varepsilon - \varepsilon_{cj})\delta_{jk} + c_{l_j}(\rho;\varepsilon - \varepsilon_{cj})\mathcal{R}_{jk}. \quad (35)$$

Thereby $\boldsymbol{\mathcal{R}}$ denotes the bare reactance matrix of the excited channels in the absence of radiative core transitions. The transformation from the bare core states to the dressed core states is mediated by the unitary trans-

formation $\mathbf{U}$ which fulfills the relation

$$\mathbf{U}^\dagger(\boldsymbol{\varepsilon}_c - \tfrac{1}{2}\boldsymbol{\Omega})\mathbf{U} = \tilde{\boldsymbol{\varepsilon}}_c. \tag{36}$$

The diagonal $N \times N$ matrix $\tilde{\boldsymbol{\varepsilon}}_c$ defines the dressed energies $\tilde{\varepsilon}_{cj} \equiv (\tilde{\boldsymbol{\varepsilon}}_c)_{jj}$. Because of our choice of ordering of channels and the fact that during radiative transitions of the ionic core the angular momentum of the Rydberg electron remains unchanged, this unitary transformation matrix is also block diagonal. Therefore, by transforming Eq. (33) it is found that

$$\{\varepsilon - [\mathbf{h} + \tilde{\boldsymbol{\varepsilon}}_c + \tilde{\mathbf{V}}(\rho)]\}\tilde{\mathbf{F}}(\rho;\varepsilon) = \tilde{\mathbf{D}}(\rho), \tag{37}$$

with $\tilde{\mathbf{V}}(\rho) = \mathbf{U}^\dagger\mathbf{V}(\rho)\mathbf{U}$, $\tilde{\mathbf{F}} = \mathbf{U}^\dagger\mathbf{F}$, and $\tilde{\mathbf{D}}(\rho) = \mathbf{U}^\dagger\mathbf{D}(\rho)$. If all channels are open an approximate fundamental system of regular solutions of the homogeneous part of Eq. (37) is given by

$$\tilde{\mathcal{F}}_{jk}(\rho;\varepsilon) = \sum_{i,l=1}^{N} \mathbf{U}^\dagger_{ji}\mathcal{F}_{il}(\rho;\varepsilon + \varepsilon_{ci} - \tilde{\varepsilon}_{cj})\mathbf{U}_{lk}. \tag{38}$$

By inserting this fundamental system of solutions into Eq. (37) it is found that

$$\begin{aligned}(\varepsilon - \mathbf{h}_{jj} - \tilde{\varepsilon}_{cj})\tilde{\mathcal{F}}_{jk}(\rho;\varepsilon) - \sum_{m=1}^{N} \tilde{\mathbf{V}}(\rho)_{jm}\tilde{\mathcal{F}}_{mk}(\rho;\varepsilon) \\ = \sum_{l,m,n,p=1}^{N} \mathbf{U}^\dagger_{jm}[\mathbf{V}(\rho)\mathbf{U}]_{ml}\mathbf{U}^\dagger_{ln}[\mathcal{F}_{np}(\rho;\varepsilon + \varepsilon_{cm} - \tilde{\varepsilon}_{cj}) \\ -\mathcal{F}_{np}(\rho;\varepsilon + \varepsilon_{cn} - \tilde{\varepsilon}_{cl})]\mathbf{U}_{pk}.\end{aligned} \tag{39}$$

Following an analogous reasoning as in the two-channel case, the right hand side of the above equation may be shown to be "close to zero" everywhere. Outside the core region the potential matrix $\mathbf{V}(\rho)$ vanishes. Inside the core region either the difference $[\mathcal{F}_{np}(\rho;\varepsilon + \varepsilon_{cm} - \tilde{\varepsilon}_{cj}) - \mathcal{F}_{np}(\rho;\varepsilon + \varepsilon_{cn} - \tilde{\varepsilon}_{cl})]$ is virtually zero or — in case at least one of the differences $\varepsilon_{cm} - \tilde{\varepsilon}_{cj}$ or $\varepsilon_{cn} - \tilde{\varepsilon}_{cl}$ is large — the matrix element $\mathbf{U}^\dagger_{jm}$ or $\mathbf{U}^\dagger_{nl}$ vanishes. This is due to the fact that only channels with approximately equal threshold energies are coupled through laser-induced core excitation.

Analogous to Eq. (23) from the asymptotic behavior of $\tilde{\boldsymbol{\mathcal{F}}}(\rho \to \infty;\varepsilon)$ the following relations are obtained for the dressed reactance and scattering matrix:

$$\tilde{\boldsymbol{\mathcal{R}}} = \mathbf{U}^\dagger\boldsymbol{\mathcal{R}}\mathbf{U}, \tag{40}$$

$$\tilde{\boldsymbol{\chi}} = \mathbf{U}^\dagger\boldsymbol{\chi}\mathbf{U}. \tag{41}$$

Furthermore, the photoionization dipole matrix elements to the dressed channels are related to the corresponding bare quantities by

$$\tilde{\mathcal{D}}^{(-)}_{g(f)j} = \sum_{i=1,N} \mathbf{U}^\dagger_{ji}\mathcal{D}^{(-)}_{g(f)i}. \tag{42}$$

Therefore, also in the multichannel case the two-photon transition amplitude is given by an expression analogous to Eq. (17) with the dressed scattering matrix and photoionization dipole matrix elements given by Eqs. (41) and (42).

III. TIME- AND ENERGY-RESOLVED SPECTROSCOPY WITH ISOLATED-CORE EXCITED ATOMS

In this section the theoretical results of Sec. II are applied to the description of the time evolution of a radial electronic Rydberg wave packet which is influenced by laser-induced Rabi oscillations of the ionic core. In part A pump-probe experiments with weak and short laser pulses are discussed. Part B is devoted to the dynamics of depletion wave packets [1,23] which are prepared by a long and intense laser field through the mechanism of power broadening. Part C complements these considerations by discussing the dependence of the dressed Rydberg state energies on the intensity of the laser inducing the core transitions. This dependence is observable in energy-resolved spectroscopic investigations.

A. Pump-probe experiments

Pump-probe experiments are a convenient method of studying the time evolution of radial electronic Rydberg wave packets [3]. In these experiments, for example, a first short and weak laser pulse prepares a radial electronic Rydberg wave packet at time t_1 by exciting Rydberg states sufficiently close to a photoionization threshold from an initially prepared energetically low lying bound state $|g\rangle$. At time t_2 a second short and weak probe pulse induces transitions from these excited Rydberg states to some other low lying bound state $|f\rangle$ or to continuum states well above threshold [4,5]. Both interactions with the laser pulses take place in a region which extends a few Bohr radii around the atomic nucleus only [1,3,23,29]. Therefore the probability of observing after the interaction with both laser pulses the atom in the final state is large whenever the initially prepared radial electronic Rydberg wave packet is close to the atomic nucleus. A slightly different method which was proposed by Noordam, Duncan, and Gallagher [6] has also been used successfully in recent experiments [10]. Thereby the two short and weak laser pulses are used for preparing two time-delayed radial electronic Rydberg wave packets whose interference is observed in the total probability of excitation.

In order to describe theoretically the Rydberg wave packet dynamics in the presence of laser-induced core coupling we derive at first a semiclassical path representation [1] for the relevant two-photon transition amplitude. For this purpose we insert expression (17) into Eq. (3) and expand the inverse matrix as a geometric series. Thus the probability of observing the atom in state $|f\rangle$ after the interaction with both short laser pulses is given by

$$|\langle f|\Psi\rangle_{t\to\infty}|^2 = \left|\int_{-\infty}^{\infty} d\varepsilon \left|\tilde{\mathcal{E}}_1(\varepsilon - \bar{\varepsilon})\right|^2 e^{-i(\varepsilon-\bar{\varepsilon})(t_2-t_1)} \sum_{i,j\in c} \tilde{\mathcal{D}}^{(-)}_{fj} \sum_{M=1}^{\infty} (e^{2\pi i\tilde{\boldsymbol{\nu}}})_{jj}[\tilde{\boldsymbol{\chi}}e^{2\pi i\tilde{\boldsymbol{\nu}}}]^{M-1}_{ji}\tilde{\mathcal{D}}^{(-)}_{gi}\right|^2 \tag{43}$$

as long as $|t_2 - t_1| \gg \tau_1, \tau_2$. The same quantity is also needed for the theoretical description of the experimental method proposed by Noordam, Duncan, and Gallagher [6].

After the initial short pulse excitation (characterized by the photoionization amplitudes $\tilde{\mathcal{D}}_{gi}^{(-)}$) only those fractions of the radial electronic Rydberg wave packet thus prepared which are excited into closed channels will return again to the core region and therefore contribute to $|\langle f \mid \Psi\rangle_{t\to\infty}|^2$. On each complete orbital round trip such a fraction acquires a phase of $e^{2\pi i\tilde{\nu}_{jj}}$. Thereby, the quantity $2\pi\tilde{\nu}_{jj}$ is the classical action which a Rydberg electron of energy $(\varepsilon - \tilde{\varepsilon}_{ci}) < 0$ accumulates during one period of motion along a purely radial Kepler orbit with zero angular momentum. Each time a fraction of the radial electronic Rydberg wave packet returns to the core region it may be scattered into one of the other dressed channels. This scattering process is described by the dressed scattering matrix $\tilde{\chi}$. In general, the moduli of the eigenvalues of $\tilde{\chi}$ are less than 1 so that at every scattering event some parts of the wave function are lost into dressed continuum channels. According to this interpretation of Eq. (43) the Mth summand of the series describes the contribution to the pump-probe signal which is associated with the Mth return of the excited Rydberg electron to the core region.

In Figs. 4–7 this general dynamical picture is illustrated for the two-channel case in which the basic effects caused by nonperturbative laser-induced core transitions can be seen most clearly. The most important parameters which determine the dynamic behavior of the wave packet are the Rabi frequency Ω_{21} of the laser-induced core transition and the difference between the quantum defects μ_1 and μ_2 of the two coupled Rydberg series. In the following examples we consider short pulse excitation from the initial state $|g\rangle$ at time t_1 to Rydberg states in the bare channel 1 around $\bar{\nu}_1 = [-2(\bar{\varepsilon} - \varepsilon_1)]^{-1/2} = 80$. This corresponds to a mean classical orbit time of $T_{orb} = 2\pi\bar{\nu}_1^3 = 77.8$ ps. A cw-laser field is applied to the atom at a time $t < t_1 - \tau_1$ and starts to induce resonant transitions (i.e., $\Delta = 0$ and $\varphi = \pi/4$) between the bare core states $|\Phi_1\rangle$ and $|\Phi_2\rangle$ as soon as the Rydberg valence electron is excited at time t_1. At time t_2 a second short laser pulse induces a transition to the final state $|f\rangle$ which is assumed to couple to channel 1 only. Therefore the quantity $|\langle f \mid \Psi\rangle_{t\to\infty}|^2$ measures the probability of finding, after preparation of an electronic Rydberg wave packet in channel 1 at time t_1, this wave packet at time t_2 again close to the ionic core and in channel 1. The envelope function for the short and weak pump and probe pulses is assumed to be of the form $\mathcal{E}_{1(2)}(t) = \mathcal{E}_{1(2)}^{(0)} \exp[-4(\ln 2)(t - t_{1(2)})^2/\tau^2]$ with pulse duration $\tau = 0.3\ T_{orb}$.

For equal quantum defects of the excited channels, i.e.,

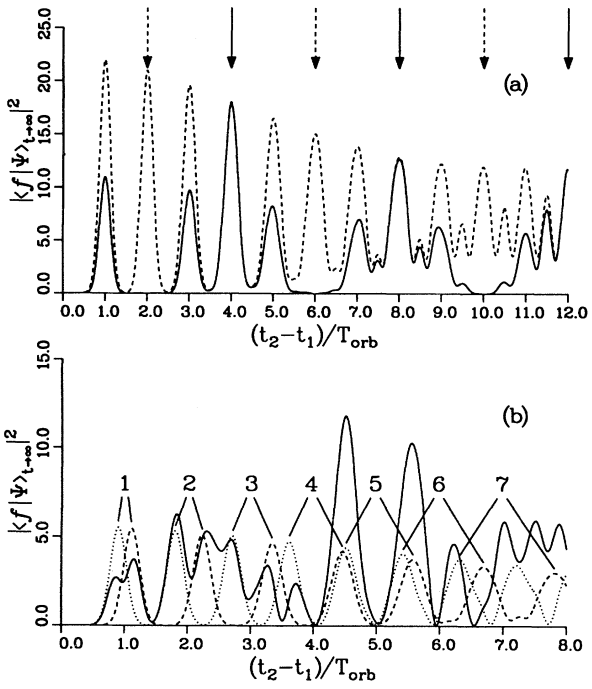

FIG. 4. Pump-probe probability $|\langle f|\Psi\rangle_{t\to\infty}|^2$ (in units of $|\mathcal{D}_{f1}^{(-)}\mathcal{E}_2^{(0)}\mathcal{D}_{g1}^{(-)}\mathcal{E}_1^{(0)}\tau|^2$) as a function of the time delay $(t_2 - t_1)$ (in units of the mean classical orbit time T_{orb}) for $\mu_1 = \mu_2 = 0.0$ and (a) $T_{Rabi} = 4\ T_{orb}$, (b) $T_{Rabi} = 0.178\ T_{orb}$. The other parameters are $\Delta = 0$, $\bar{\nu}_1 = 80$, $T_{orb} = 77.8$ ps and $\tau = 0.3\ T_{orb}$. The dashed curve in Fig. 4(a) shows the pump-probe probability in absence of laser-induced core coupling ($\Omega_{21} = 0$). The dashed and dotted curves in Fig. 4(b) show the individual probability contributions of the two wave packet fractions (see text). The number M ($M = 1, \ldots, 7$) indicates the Mth recurrence.

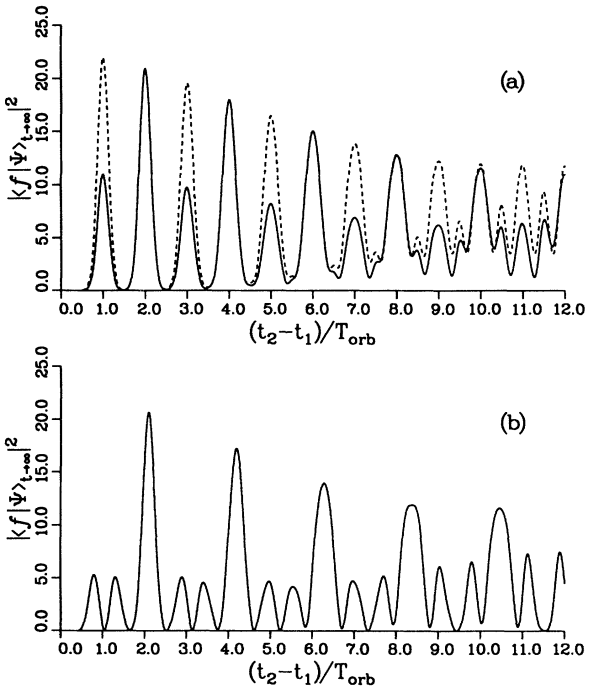

FIG. 5. $|\langle f|\Psi\rangle_{t\to\infty}|^2$ for $\mu_1 = 0.0$, $\mu_2 = 0.5$ and (a) $T_{Rabi} = 4\ T_{orb}$, (b) $T_{Rabi} = 0.081\ T_{orb}$. Other parameters as in Fig. 4. The dashed curve in Fig. 5(a) shows the pump-probe probability for $\Omega_{21} = 0$.

$\mu_1 = \mu_2$, the scattering matrix $\tilde{\chi}$ is a multiple of the unit matrix. This implies that in this case the excited Rydberg electron is not shaken up by the laser-induced core transitions. Consequently, no scattering takes place between the dressed channels. After the initial excitation which occurs with equal amplitude into both dressed channels the fractions of the prepared wave packet evolve independently from each other. This can be seen clearly in Fig. 4(b) where $T_{Rabi} = 2\pi/\Omega_{21} = 0.178\ T_{orb}$. Due to the ac-Stark splitting of the channel thresholds the two fractions have orbit times 1.12 T_{orb} and 0.90 T_{orb}, respectively. Their indivual contributions to the pump-probe signal are indicated by the dashed and dotted curves in Fig. 4(b). They display the independent evolution of the fractions. The structure of the peaks in $|\langle f \mid \Psi\rangle_{t\to\infty}|^2$ arises from the quantum mechanical interference of these contributions.

Interference effects do not only arise for the case of strong laser-induced coupling of the core states, i.e., $T_{Rabi} \ll T_{orb}$, but also for weak ICE processes with

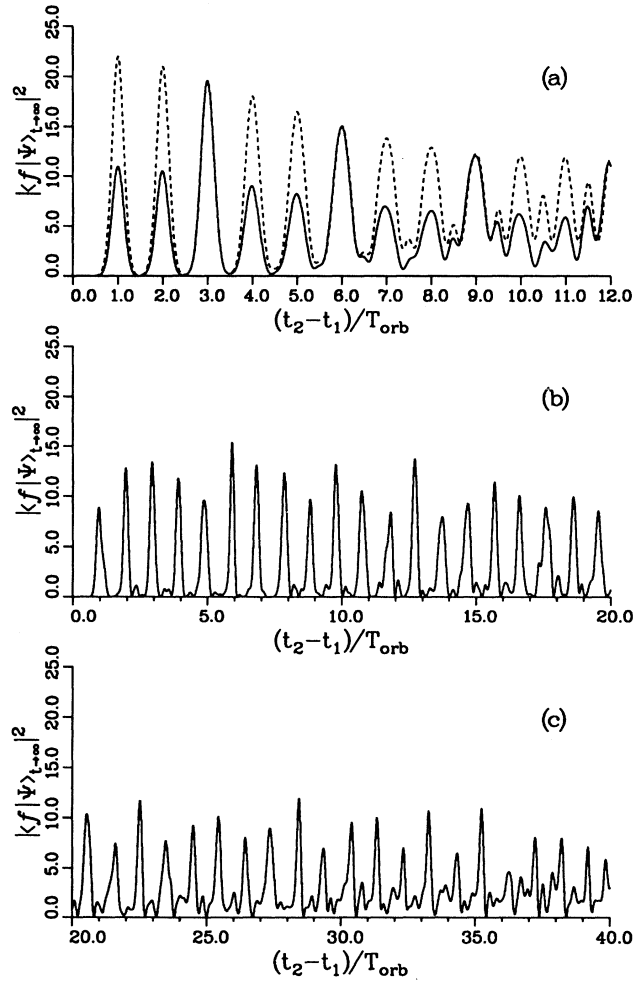

FIG. 6. $|\langle f|\Psi\rangle_{t\to\infty}|^2$ for $\mu_1 = 0.0$, $\mu_2 = 0.25$ and (a) $T_{Rabi} = 4\ T_{orb}$, (b), (c) $T_{Rabi} = 0.195\ T_{orb}$. Other parameters as in Fig. 4 besides $\tau = 0.16\ T_{orb}$ in (b) and (c). The dashed curve in Fig. 6(a) shows the pump-probe probability for $\Omega_{21} = 0$.

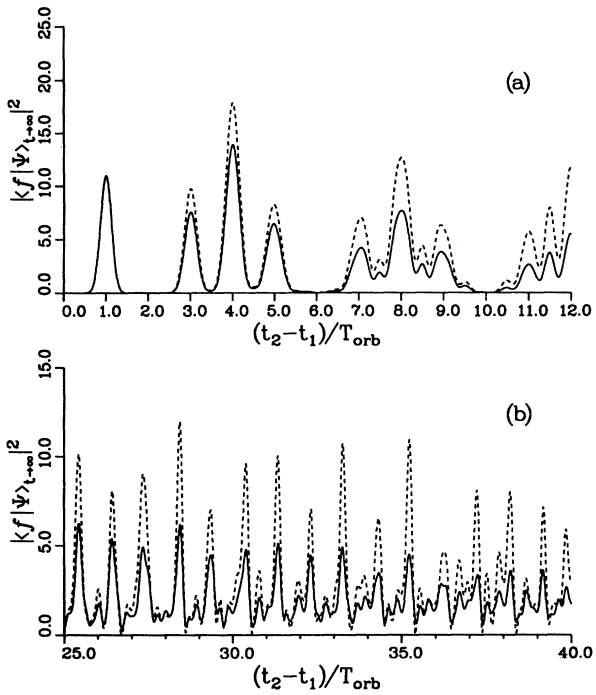

FIG. 7. Influence of autoionization on the pump-probe probability. The dashed curves are the same as in Figs. 4(a) and 6(c), respectively. The full curves show the pump-probe probability for Im $\mu_2 = 0.01$.

$T_{Rabi} \gg T_{orb}$. In this latter case the two fractions of the electronic Rydberg wave packet which are prepared by the short and weak laser pulse in the dressed channels have almost the same orbit time so that they return to the ionic core almost simultaneously. However, the phases which they accumulate during each complete orbital round trip differ by an amount of approximately $\Delta S = T_{orb}\ |\Omega_{21}|$. This phase difference leads to a modulation of the magnitude of the recurrence peaks in the pump-probe transition probability $|\langle f \mid \Psi\rangle_{t\to\infty}|^2$ with an envelope function approximately given by $\cos^2\ [|\Omega_{21}|(t_2 - t_1)]$. These modulations reflect the Rabi oscillations of the ionic core: whenever the core is in (bare) state 2 or 1 the overlap between the excited radial electronic Rydberg wave packet and state $|f\rangle$ (and therefore the pump-probe probability) vanishes or is maximal. This behavior is exemplified in Fig. 4(a) for the case of $T_{Rabi} = 4\ T_{orb}$. The dashed (full) arrows indicate the times when $\cos^2\ [|\Omega_{21}|(t_2 - t_1)]$ vanishes (is maximal). For the sake of comparison the dashed curve shows the time evolution of $|\langle f \mid \Psi\rangle_{t\to\infty}|^2$ in the absence of laser-induced core transitions, i.e., for $\Omega_{21} = 0$.

In Figs. 5 the other extreme case, i.e., maximal difference in quantum defects $\mu_2 - \mu_1 = 0.5$, is considered. According to Eqs. (25) and (26) in this case the scattering matrix is completely off-diagonal and is given by

$$\tilde{\chi} = e^{2\pi i \mu_1} e^{i\pi} \begin{pmatrix} 0 & 1 \\ 1 & 0 \end{pmatrix}.$$

Therefore the shakeup of the Rydberg electron caused

by the laser-induced core transitions is so effective that at each return to the core region the two fractions of the electronic Rydberg wave packet which evolve in the dressed channels are scattered from one channel into the other with a probability of unity. This scattering mechanism is clearly visible in Fig. 5(a) in which a case of weak laser-induced core coupling with $T_{Rabi} = 4\ T_{orb}$ is shown. Therefore the orbit times of the two fractions of the electronic Rydberg wave packet in the dressed channels are approximately equal and they return to the core almost simultaneously. At odd multiples of T_{orb}, for example at the first return, the contributions of the two fractions to the pump-probe probability cancel each other partially because their accumulated phases differ by an amount $|\Delta S| = T_{orb}|\Omega_{21}| = \pi/2$. At the same time, however, each fraction is scattered completely from one dressed channel into the other one. Therefore at the next return to the core region (at an even multiple of T_{orb}) they both have accumulated the same phase and consequently their contributions to $|\langle f \mid \Psi\rangle_{t\to\infty}|^2$ add constructively.

In Fig. 5(b) a case of strong laser-induced core coupling is considered with $T_{Rabi} = 0.081\ T_{orb}$. This implies a larger separation of the thresholds of the dressed channels and thus a significant difference in the orbit times of the wave-packet fractions which are prepared initially in the dressed channels. At odd multiples of T_{orb} two-peaked maxima are observed which represent the temporally separated returns of the two fractions. However, at each return to the core region the faster part of the wave packet is scattered into the dressed channel with the longer return time and vice versa. Therefore at even multiples of T_{orb} both fractions reach the core simultaneously and their contributions to the pump-probe probability add constructively giving rise to one-peaked large maxima.

In the case of an intermediate difference in quantum defects $\mu_2 - \mu_1 = 0.25$ the scattering matrix is of the form

$$\tilde{\boldsymbol{\chi}} = \frac{1}{\sqrt{2}} e^{2\pi i \mu_1} e^{i\pi/4} \begin{pmatrix} 1 & e^{i\pi/2} \\ e^{i\pi/2} & 1 \end{pmatrix}.$$

This implies that in the course of its successive returns to the core region the electronic Rydberg wave packet is split up into a rapidly growing number of individual fractions with almost equal amplitudes. Therefore in general the behavior of $|\langle f \mid \Psi\rangle_{t\to\infty}|^2$ is more complicated than in the above examples. If, for example, Ω_{21} is chosen so that $T_{Rabi} = 4\ T_{orb}$ it can be seen from Fig. 6(a) that the contributions of the fractions of the electronic wave packet add constructively at every third return to the core region. This behavior is distinctly different from the ones displayed in the corresponding Figs. 4(a) and 5(a).

In the case of strong laser-induced core coupling, i.e., $T_{Rabi} > T_{orb}$, $|\langle f \mid \Psi\rangle_{t\to\infty}|^2$ generally shows a very complicated behavior without any easily recognizable pattern. This is due to the many contributing wave packet fractions with different recurrence times. However, for certain values of Ω_{21} a long-time suppression of the dispersion of the pump-probe probability can be observed. This effect is especially pronounced for shorter pulse durations. If we take $\tau = 0.16\ T_{orb}$, for example, then in the absence of laser-induced core transitions, i.e., with $\Omega_{21} = 0$, the single maxima in the pump-probe probability at integer values of T_{orb} would disappear completely due to the dispersion of the wave packet for pump-probe delays greater than 6 T_{orb}. In the presence of laser-induced core transitions with $\Omega_{21} = 1.0 \times 10^{-5}$ a.u., however, one observes sharp and pronounced maxima with a temporal separation of approximately T_{orb} for times as long as 35 T_{orb} [Figs. 6(b),(c)]. This effect was also observed for other values of the excited quantum number $\bar{\nu}_1$. It is due to interferences between the many contributing fractions of the electronic Rydberg wave packet which evolve in the dressed channels.

In the examples discussed so far, only the idealized two-channel model introduced in part A of Sec. II has been considered for the sake of clarity. More realistic excitation schemes with N channels involved can be dealt with by using the results derived in part B of Sec. II. However, effects of autoionization of channel 2, which have always to be taken into account in realistic situations, can also be described within the framework of the two-channel approximation by adding to the quantum defect μ_2 an imaginary part which is equal to one half of the scaled autoionization linewidth. Examples of corresponding calculations of $|\langle f \mid \Psi\rangle_{t\to\infty}|^2$ are shown in Fig. 7. There, Im μ_2 is taken equal to 0.01 which is a typical value for these kinds of autoionization processes [30]. These figures indicate that, in general, autoionization will leave the qualitative features of the pump-probe probability unchanged and will only lead to minor quantitative deviations from the nonautoionizing two-channel case. The most prominent of these deviations is a decrease in the height of the recurrence peaks. It is due partly to the loss of probability into the continuum channels and partly also to destructive interferences between the fractions of the wave packet which evolve in the dressed channels.

B. Time evolution of depletion wave packets

A radial electronic Rydberg wave packet can also be prepared by exciting the initial state $|g\rangle$ with an intense and long laser pulse provided the state $|g\rangle$ is depleted on a time scale small in comparison with the mean classical orbit time of the excited Rydberg states [23]. Physically this situation is different from the case of weak and short pulses considered in part A because now the initially prepared wave packet propagates also under the influence of this additional cw-laser field. The investigation of this kind of excitation process is of interest as it represents a basic constituent for possible further applications of ICE-modified wave packet dynamics, for example in atom optics [31]. For the sake of simplicity we restrict the following discussion to the two-channel approximation; however, it may be generalized immediately to the N-channel case.

We take the laser field exciting the initial state $|g\rangle$ resonantly to Rydberg states in channel 1 close to the photoionization threshold to be given by $\mathbf{E}_1(t) = \mathcal{E}_1 \mathbf{e}_1 e^{-i\omega_1 t} + \text{c.c.}$ The laser-induced core excitation is again achieved by the laser field $\mathbf{E}(t)$. Under these cir-

cumstances the probability of finding at time t the atom in its initial state $|g\rangle$ is given by [23],

$$a_g(t) = \frac{1}{2\pi} \int_{-\infty+i0}^{+\infty+i0} dz\, e^{-izt} a_g(z)\,, \tag{44}$$

with the Laplace transform

$$a_g(z) = \int_0^\infty dt\, e^{i(z+i0)t} a_g(t) = i[z - \varepsilon_g - T_{gg}(z+\omega_1)]^{-1}. \tag{45}$$

This Laplace transform can be expressed in the form of a semiclassical path representation,

$$a_g(z) = a_g^{(0)}(z) + 2\pi a_g^{(0)}(z) \sum_{i,j\in c} \tilde{\mathcal{D}}_{gj}^{(-)} \left(e^{2\pi i\tilde{\boldsymbol{\nu}}}\right)_{jj} \times \sum_{M=1}^{\infty} [\boldsymbol{\Xi}(z) e^{2\pi i\tilde{\boldsymbol{\nu}}}]_{ji}^{M-1} \tilde{\mathcal{D}}_{gi}^{(-)} a_g^{(0)}(z) \,|\mathcal{E}_1|^2 \tag{46}$$

with

$$a_g^{(0)}(z) = i(z + \omega_1 - \bar{\varepsilon} + i\Gamma/2)^{-1}$$

and

$$\boldsymbol{\Xi}_{jk}(z) = \tilde{\boldsymbol{\chi}}_{jk} + 2\pi i \tilde{\mathcal{D}}_{gj}^{(-)} a_g^{(0)}(z) \tilde{\mathcal{D}}_{gk}^{(-)\,T} \,|\mathcal{E}_1|^2\,.$$

Again the subscript c denotes restriction of the sum to closed channels only.

The dynamical interpretation of Eqs. (44) and (46) is very similar to the one given for Eq. (43): the first term in Eq. (46) describes the initial depletion of state $|g\rangle$ by the cw-laser field $\mathbf{E}_1(t)$. Thereby this laser field leads to a quadratic Stark shift $\delta\omega$ between the initial state $|g\rangle$ and the excited Rydberg states. This shift has been absorbed in the definition of the mean excited energy $\bar{\varepsilon} = \varepsilon_g + \omega_1 + \delta\omega$. The rate $\Gamma = 2\pi \sum_{j=1,2} |\tilde{\mathcal{D}}_{gj}^{(-)} \mathcal{E}_1|^2$ equals the ionization rate which describes ionization from state $|g\rangle$ to continuum states close to threshold perturbatively. Its inverse determines the time scale at which the initially prepared state $|g\rangle$ is depleted by the intense laser field $\mathbf{E}_1(t)$. An electronic Rydberg wave packet is prepared in this excitation process if $1/\Gamma$ is less than the mean classical orbit time of the excited Rydberg states. The remaining contributions on the right hand side of Eq. (46) describe effects which arise from repeated returns of the excited Rydberg electron to the ionic core region. If the excited Rydberg electron enters the core region again it can be de-excited by the field $\mathbf{E}_1(t)$ into the initial state $|g\rangle$. In this way the initial state probability $a_g(t)$ is increased. The Mth member of the sum in Eq. (46) represents the contribution of this de-excitation process which takes place at the Mth return of the excited Rydberg electron to the core region. Alternatively, however, at each of these returns the excited Rydberg electron can also be scattered in the presence of the cw-laser fields from dressed channel k into the dressed channel j. This process is characterized by the scattering matrix element $\boldsymbol{\Xi}_{jk}$. There are two contributions to this scattering process. One of them is described by $\tilde{\boldsymbol{\chi}}_{jk}$ and originates from the shakeup process caused by the Rabi oscillations of the ionic core which are induced by the laser field $\mathbf{E}(t)$. The second one is described by the energy-dependent term $2\pi i \tilde{\mathcal{D}}_{gj}^{(-)} a_g^{(0)}(z) \tilde{\mathcal{D}}_{gk}^{(-)} |\mathcal{E}_1|^2$. This expression describes laser-assisted scattering events induced by the cw-laser field $\mathbf{E}_1(t)$ by de-exciting the Rydberg electron from channel k into state $|g\rangle$ and re-exciting it again into channel j.

In Fig. 8 two examples for the temporal behavior of the initial state probability $|a_g(t)|^2$ are shown for the case of two nonautoionizing coupled channels. The parameters $\mu_2 - \mu_1$, $\bar{\nu}_1$, Ω_{21}, and Δ are the same as in Figs. 4(a) and 5(b), respectively. The intensity of the laser field $\mathbf{E}_1(t)$ is chosen so that $1/\Gamma = 0.05\ T_{orb}$. A comparison of Figs. 8(a) and 8(b) with Figs. 4(a) and 5(b), respectively, shows that the effects originating from the laser-assisted scattering of the Rydberg electron inside the core region lead to significant quantitative changes of the dynamics. However, in Fig. 8(a) modulations of the recurrence peaks due to Rabi oscillations of the ionic core can still be recognized. In Fig. 8(b) the splitting of the wave function into two parts which is due to the ICE-induced ac-Stark splitting of the channel thresholds is clearly visible for $t \simeq T_{orb}$.

C. Dressed state energies

In this subsection the dependence of the energies of the dressed Rydberg states, i.e., the eigenstates of the Hamiltonian of Eq. (6), on the strength of the laser-induced core coupling is discussed. In this way a complementary

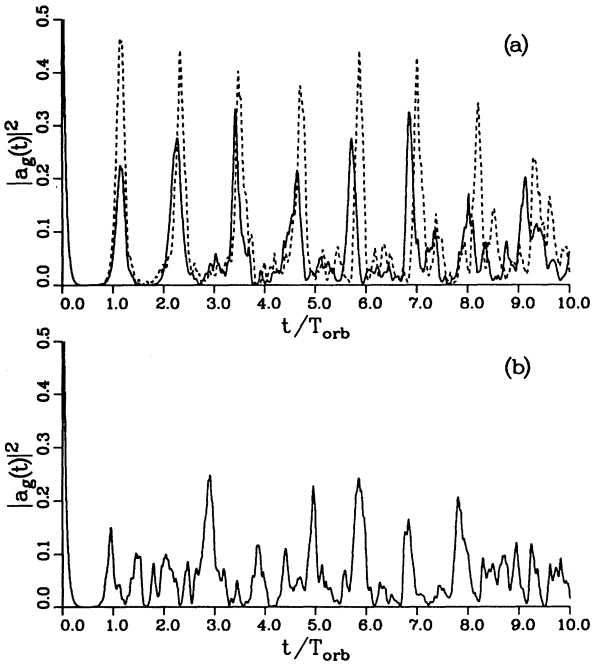

FIG. 8. Initial state probability as a function of time for long pulse excitation of $|g\rangle$: (a) $\mu_1 = \mu_2 = 0.0$ and $T_{Rabi} = 4\ T_{orb}$ (dashed curve: $\Omega_{21} = 0$), (b) $\mu_1 = 0.0$, $\mu_2 = 0.5$ and $T_{Rabi} = 0.081\ T_{orb}$. The other parameters are $1/\Gamma = 0.05\ T_{orb}$, $\Delta = 0$, $\bar{\nu}_1 = 80$.

view of the mixing of the Rydberg series by the laser field is obtained. We consider the two-channel case as shown in Fig. 1. The dressed state energies $\tilde{\varepsilon}_n$ are determined by the condition

$$\det(\tilde{\boldsymbol{\chi}} - e^{-2\pi i\tilde{\boldsymbol{\nu}}}) = 0. \tag{47}$$

In Figs. 9 these dressed energies are shown as a function of the laser-induced core coupling strength Ω_{21} for various differences of the quantum defects μ_1 and μ_2 and resonant laser-induced core coupling $\Delta = 0$.

Experimentally, such spectra can be obtained by means of energy-resolved spectroscopy in a context as described at the end of Sec. II A. There it was mentioned that in the case of excitation of the initially prepared

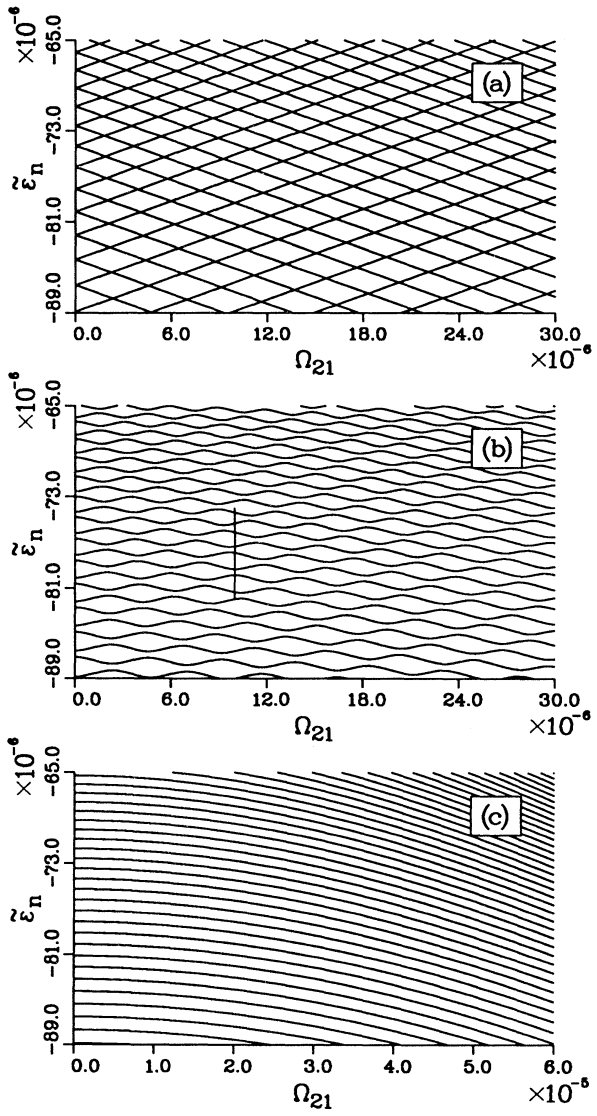

FIG. 9. Energies of dressed Rydberg states (relative to the "bare" threshold ε_{c1}, compare Fig. 1) as a function of Ω_{21} for resonant coupling $\Delta = 0$ and (a) $\mu_1 = \mu_2 = 0.0$, (b) $\mu_1 = 0.0$, $\mu_2 = 0.25$, (c) $\mu_1 = 0.0$, $\mu_2 = 0.5$. The vertical line in Fig. 9(b) indicates the excited energy region used in Fig. 6(b),(c).

state $|g\rangle$ to the bare channels 1 and 2 (where channel 2 is slightly autoionizing) by two cw-laser fields with amplitudes $\mathcal{E}_1$ and $\mathcal{E}$ the depletion rate Γ of state $|g\rangle$ is given by $\Gamma = -2\,|\mathcal{E}_1|^2\ \mathrm{Im}\ T_{gg}(\varepsilon_g + \omega_1)$. The dressed state energies are thus found by observing the position of the resonances as a function of the laser frequency ω_1.

In Fig. 9(a) the case $\mu_1 = \mu_2$ is shown. This spectrum can be understood within the picture of two independent dressed channels which was also used for the discussion of the corresponding pump-probe probabilities (Fig. 4). Each dressed state can thus be assigned unambiguously to one of the dressed channels. The energies of the dressed states exhibit directly the ac-Stark splitting of the core states. The spectrum is therefore divided into two groups of linearly ascending and descending energy levels which intersect each other without avoided crossings.

For a difference in quantum defects of $\mu_2 - \mu_1 = 0.25$ [Fig. 9(b)] the main feature of the preceding diagram, namely the two groups of linearly ascending and descending energy levels, is still recognizable. However, due to the channel mixing which is caused by the radiative core coupling the energy levels show well-pronounced avoided crossings. There are no obviously remarkable structures in the region of the spectrum (indicated by the vertical line) which corresponds to the excited energy region used in Figs. 6(b),(c) where the dispersion of the pump-probe probability was strongly suppressed.

Figure 9(c) shows the dressed energy spectrum for the case of maximal difference in quantum defects, i.e., $\mu_2 - \mu_1 = 0.5$. Therefore effects which originate from the shake-up of an excited Rydberg electron by laser-induced core transitions are expected to be large. The corresponding states cannot be assigned to a single channel. For $\Omega_{21} = 0$ each state has approximately equal distance in energy to both its neighbors and due to the level repulsion it tends to keep this maximum separation to both sides also when the coupling strength Ω_{21} is increased. This explains the almost horizontal direction of the curves for small values of Ω_{21}. For large enough values of Ω_{21}, however, all levels are gradually pushed downwards because they must always stay below the lower threshold of the Rydberg series which has energy $\varepsilon_1 - \frac{1}{2}\,|\Omega_{21}|$. Figure 9(c) also gives an alternative explanation for the dynamical behavior shown in Fig. 5(b). As neighboring levels are separated by $1/2{*}1/\nu^3$, approximately, an electronic Rydberg wave packet should regain its initial shape at multiples of $2 \times T_{orb}$. This explains the well pronounced recurrence peaks which appear at even multiples of T_{orb} in Fig. 5(b).

IV. CONCLUSION

Based on the concept of photon-dressed core channels and on MQDT an analytical approach for the description of the dynamics of an electronic Rydberg wave packet under the influence of nonperturbative laser-induced core transitions has been developed. We have put the emphasis mainly on the discussion of pump-probe experiments with short and weak laser pulses. With the help

of a semiclassical path representation, the dynamics of the Rydberg electron could be described in a concise way thus yielding the picture of a Rydberg wave packet which is shaken up by the laser-induced core transitions whenever it penetrates the core region. The discussion of the dependence of these dynamics on the relevant physical parameters showed that by an appropriate choice of the atomic excitation scheme and the laser characteristics one has a great variety of new possibilities to influence the dynamics of a radial electronic Rydberg wave packet. The wave packet can be used to probe the time evolution of the Rabi oscillations of the core electron [compare with Fig. 4(a)] or vice versa the Rabi oscillations of a core electron might be used to control the dynamics of the wave packet [as in Figs. 6(b),(c)].

A major problem for the observation of effects due to nonperturbative core transitions in energy-resolved spectroscopy is the necessity of driving the ICE transitions by rather strong laser fields: on the one hand the Rabi frequency should exceed the mean level spacing of the excited Rydberg states ($\bar{\nu}^3\Omega > 1$), but on the other hand one has to excite Rydberg states with not too large quantum numbers due to the finite resolution of the probe laser [19]. In time-dependent experiments, however, the wave packet dynamics is modified significantly already for weak core excitations ($\bar{\nu}^3\Omega < 1$), and wave packets with a rather large mean quantum number can be prepared. The effects of nonperturbative core transitions should therefore be observable with significantly lower laser intensities.

ACKNOWLEDGMENTS

This work was supported by the SFB 276 of the Deutsche Forschungsgemeinschaft.

[1] G. Alber and P. Zoller, Phys. Rep. **199**, 231 (1991).
[2] J. Parker and C. R. Stroud, Jr., Phys. Rev. Lett. **56**, 716 (1986).
[3] G. Alber, H. Ritsch, and P. Zoller, Phys. Rev. A **34**, 1058 (1986).
[4] D. R. Meacher, P. E. Meyler, I. G. Hughes, and P. Ewart, J. Phys. B **24**, L63 (1991).
[5] J. A. Yeazell and C. R. Stroud, Jr., Phys. Rev. A **43**, 5153 (1991).
[6] L. D. Noordam, D. I. Duncan, and T. F. Gallagher, Phys. Rev. A **45**, 4734 (1992).
[7] R. Bluhm and V. A. Kostelecký, Phys. Rev. A **49**, 4628 (1994).
[8] I. Sh. Averbukh and N. F. Perelman, Phys. Lett. A **139**, 449 (1989); M. Fleischhauer and W. P. Schleich, Phys. Rev. A **47**, 4258 (1993); P. A. Braun and V. I. Savichev, *ibid.* **49**, 1704 (1994).
[9] G. Alber, Phys. Rev. A **40**, 1321 (1989); Z. Phys. D **14**, 307 (1989); M. W. Beims and G. Alber, Phys. Rev. A **48**, 3123 (1993).
[10] J. A. Yeazell, G. Raithel, L. Marmet, H. Held, and H. Walther, Phys. Rev. Lett. **70**, 2884 (1993); J. Wals, H. H. Fielding, J. F. Christian, L. C. Snoek, W. J. van der Zande, and H. B. van Linden van den Heuvell, *ibid.* **72**, 3783 (1994).
[11] W. E. Cooke, T. F. Gallagher, S. A. Edelstein, and R. M. Hill, Phys. Rev. Lett. **40**, 178 (1978).
[12] See, for example, R. R. Jones and T. F. Gallagher, Phys. Rev. A **42**, 2655 (1990); R. R. Jones, Panming Fu, and T. F. Gallagher, *ibid.* **44**, 4265 (1991); P. Camus, J.-M. Leconte, C. R. Mahon, P. Pillet, and L. Pruvost, J. Phys. (France) II **2**, 715 (1992).
[13] X. Wang and W. E. Cooke, Phys. Rev. Lett. **67**, 976 (1991).
[14] X. Wang and W. E. Cooke, Phys. Rev. A **46**, R2201 (1992).
[15] X. Wang and W. E. Cooke, Phys. Rev. A **46**, 4347 (1992).
[16] J. G. Story, D. I. Duncan, and T. F. Gallagher, Phys. Rev. Lett. **71**, 3431 (1993).
[17] R. R. Jones and P. H. Bucksbaum, Phys. Rev. Lett. **67**, 3215 (1991).
[18] H. Stapelfeldt, D. G. Papaioannou, L. D. Noordam, and T. F. Gallagher, Phys. Rev. Lett. **67**, 3223 (1991).
[19] F. Robicheaux, Phys. Rev. A **47**, 1391 (1993).
[20] R. Grobe and J. H. Eberly, Phys. Rev. A **48**, 623 (1993).
[21] M. J. Seaton, Rep. Prog. Phys. **46**, 167 (1983).
[22] U. Fano and A. R. P. Rau, *Atomic Collisions and Spectra* (Academic Press, New York, 1986).
[23] G. Alber and P. Zoller, Phys. Rev. A **37**, 377 (1988).
[24] W. A. Henle, H. Ritsch, and P. Zoller, Phys. Rev. A **36**, 683 (1987).
[25] S. A. Bhatti, C. L. Cromer, and W. E. Cooke, Phys. Rev. A **24**, 161 (1981).
[26] N. H. Tran, P. Pillet, R. Kachru, and T. F. Gallagher, Phys. Rev. A **29**, 2640 (1984).
[27] A. Dalgarno and J. T. Lewis, Proc. R. Soc. London, Ser. A **233**, 70 (1955).
[28] J. Dubau and M. J. Seaton, J. Phys. B **17**, 381 (1984).
[29] A. Giusti-Suzor and P. Zoller, Phys. Rev. A **36**, 5178 (1987).
[30] W. Sandner, Comments At. Mol. Phys. **20**, 171 (1987).
[31] G. Alber, W. T. Strunz, and O. Zobay, Mod. Phys. Lett. B **8**, 1461 (1994).